REVIEW

Check for updates

Rational design of bifunctional conjugated microporous polymers

Yanpei Song, Pui Ching Lan, Kyle Martin and Shengqian Ma [ID] *

Conjugated microporous polymers (CMPs) are an emerging class of porous organic polymers that combine π-conjugated skeletons with permanent micropores. Since their first report in 2007, the enormous exploration of linkage types, building units, and synthetic methods for CMPs have facilitated their potential applications in various areas, from gas separations to energy storage. Owning to their unique construction, CMPs offer the opportunity for the precise design of conjugated skeletons and pore environment engineering, which allow the construction of functional porous materials at the molecular level. The capability to chemically alter CMPs to targeted applications allows for the fine adaptation of functionalities for the ever-changing environments and necessities. Bifunctional CMPs are a branch of functionalized CMPs that have caught the interest of researchers because of their inherent synergistic systems that can expand their applications and optimize their performance. This review discusses the rational design and synthesis of bifunctional CMPs and summarizes their advanced applications. To conclude, our own perspective on the research prospects of these types of materials is outlined.

1. Introduction

Materials bearing permanent porosities are considered porous materials, which have drawn wide attention as an attractive platform for their advanced applications in the various fields of science and technology. Porosity, however, is not a new concept and has long existed in nature, such as cavities in the structure of charcoal. Synthetic porous materials, which also possess permanent porosities, are constantly attracting attention from scientists to discover their potential applications due to their feasible functionalization. In the past several decades, a variety of synthetic porous materials have emerged, resulting in the explosion of material design. Zeolites and mesoporous silicates are traditional porous materials with inorganic open frameworks which are still widely used in industrial production in modern times.[1–4] In addition, another type of prevalent inorganic containing porous materials are metal–organic frameworks (MOFs) or porous coordination polymers (PCPs) representing one of the most attractive classes of porous materials nowadays.[5–9] As a result of the rapid development of module construction, MOFs held together by coordination bonds can be connected in a predictable manner. This then allows for the feasibility to manipulate the functional units and spatial structures of the framework, thereby allowing control over the internal surface engineering and functionalization of

Department of Chemistry, University of North Texas, 1508 W Mulberry St, Denton, TX 76201, USA. E-mail: shengqian.ma@unt.edu

Yanpei Song received his BS degree from the Beijing University of Chemical Technology in 2017. He is currently a Ph.D. candidate at the University of North Texas under the supervision of Prof. Shengqian Ma. His current research interests focus on the development of functional porous organic polymers for environmental remediation and precious metal recovery.

Pui Ching Lan received his BS degree from the University of California, Berkeley in 2014. He then worked for three years with the Material Science Division at Lawrence Livermore National Laboratory before starting his Ph.D. career with Dr Shengqian Ma at the University of North Texas. His research focuses on the synthesis and the characterization of novel functional covalent organic frameworks for biomass valorization and energy storage.

MOFs.[10–13] In sharp contrast to the inorganic or inorganic-hybrid porous materials, there is also a collection of advanced organic materials with permanent nano-porosities, which are constructed by the infinite connections of covalent bonds between organic units, and these materials are classified as porous organic materials.

In the past two decades, covalent organic frameworks (COFs),[14–18] covalent triazine frameworks (CTFs),[19–23] porous organic polymers (POPs),[24–27] hyper crosslinked polymers (HCPs),[28–31] porous aromatic frameworks (PAFs)[32–35] and conjugated microporous polymers (CMPs)[36–39] have been introduced, and most of them are amorphous and disordered networks except for COFs and a small number of CTFs. These porous organic materials possess various structural features and linking knots; they, however, are all constructed from light elements with high porosity, excellent stability, and facile functionalization. Among these porous organic materials, CMPs are unique ones because of their extended π-conjugated skeletons, which build porous 3D networks of CMPs. Based on this concept, CTFs can also be considered as a subclass of CMPs because of their microporous properties and extended π-conjugation in the structure, although there are many differences in the construction between them and traditional CMPs.

The initial effort to construct CMPs was made by Cooper and co-workers when they reported the first three CMP networks.[40] To achieve the π-conjugated skeletons, these CMPs were synthesized *via* palladium-catalyzed Sonogashira–Hagihara cross-coupling to ensure that the network was based on a 1,3,5-substituted benzene node connected by rigid phenyleneethynylene struts. The network CMP-1 was obtained from the cross-coupling of 1,3,5-triethynylbenzene and 1,4-diiodobenzene representing an amorphous 3D structure. CMP-1 exhibited microporous properties, as revealed by the N_2 sorption isotherms collected at 77 K, with a Brunauer–Emmett–Teller (BET) surface area of 834 m^2 g^{-1}. Other CMPs, CMP-2, and CMP-3, which are also based on the integration of C3 + C2 topological units into CMPs reveal similar 3D structures as CMP-1 with the BET surface areas of 634 and 552 m^2 g^{-1}, respectively. Cooper's group also was the first to synthesize a soluble CMP network in 2012 *via* the introduction of *tert*-butyl-functionalized groups to the skeleton to obtain the hyperbranched CMPs, and thus handling the CMP in a state other than solid.[41] The resultant CMP could dissolve in a specific solvent and then cast as thin films, demonstrating the promising application in the separation of gases. Later, Patra[42] and Hu[43] *et al.* by building upon this approach reported another two examples of the casting of thin films from soluble CMPs and their applications in light emission and fluorescence detection. These successful attempts stimulated the growth of CMP materials from the building block design to the synthetic methods. Due to the diversity of chemical reactions, numerous coupling units are designed for the application of interest, which also expands the synthetic reactions for the construction of CMP networks, including Sonogashira–Hagihara reaction,[44] Suzuki cross-coupling reaction,[45,46] Yamamoto reaction,[47] Heck reaction,[48] Friedel–Crafts reaction,[49,50] phenazine ring fusion reaction,[51,52] oxidative coupling reaction,[53] Schiff-base reaction[54,55] and cyclotrimerization reaction (Fig. 1).[56,57]

2. Design and synthesis of bifunctional CMPs

CMPs with their unique π-conjugated skeletons and permanent micropores in structure demonstrate the great potential in advanced applications which can be designed at the molecular level and constructed according to researchers' intention. With the advent of CMPs, they have been applied for gas storage and separation due to their inherent advantages such as high

Kyle Martin received his BS degree from University of North Texas in 2021, and then joined the research group of Prof. Shengqian Ma as a Ph.D. student at the University of North Texas. His current research interests focus on the water purification and precious metal extraction.

Shengqian Ma obtained his BS degree from Jilin University, China in 2003, and graduated from Miami University (Ohio) with a Ph.D. degree in 2008. After finishing a two-year Director's Postdoctoral Fellowship at Argonne National Laboratory, he joined the Department of Chemistry at the University of South Florida as an Assistant Professor in 2010; he was promoted to Associate Professor with early tenure in 2015 and to a Full Professor in 2018. In August 2020, he joined the University of North Texas as the Robert A. Welch Chair in Chemistry. His current research interest focuses on the development of functional porous materials including metal–organic frameworks (MOFs), covalent organic frameworks (COFs), porous organic polymers (POPs), and microporous carbon materials for energy, biological, environmental-related applications.

Fig. 1 Schematic representation of reactions for the synthesis of CMPs.

surface areas and rigid π-conjugated structures.[58–62] Functionalizing CMPs beyond their intrinsic properties represents a foreseeable approach to addressing critical challenges such as heterogeneous catalysis,[63–67] photocatalysis,[65–67] light emittance,[68–70] environmental remediation,[71–74] chemical sensing,[75–78] and energy storage.[79–84] In addition, bifunctional CMPs with multiple active sites or functionalities can strengthen their performance with the close cooperation of diverse assistant groups and improve the issue of low efficiency in single-functional CMPs that may hinder their practical applications. In this section, we review the design and synthesis of bifunctional CMPs with a rational evaluation of these strategies.

2.1 Design principles

The routes to design and synthesize a CMP network are full of challenges, which require researchers to have careful consideration for network structures and appropriate methods to include functionalities in CMPs. Generally, the establishment of a CMP network is driven by their skeleton architecture or potential applications with well-designed functional groups. Sometimes it is also necessary to address a task with the combination of these factors together. It is well known that the self-condensation of the homo-coupling of single building blocks occurs earlier than that of CMPs, such as in the first success for the construction of COF-1, which was obtained by the self-condensation of 1,4-benzene diboronic acid and had

crystalline structure and permanent porosity.[14] However, the discovery of such porous organic polymers is limited by their confined establishment of skeletons, which are merely the infinite duplication of homo-monomers. Thus, an important principle for designing functional CMPs, especially the bifunctional CMP, is that diverse building monomers with two or more active groups are necessary to endow the resultant CMP with accessible functionalities beyond their π-conjugated skeletons. According to this principle, the rational design of monomers and accessible functionalizing methods are indispensable for the consideration of researchers. After the first introduction of the CMP network,[40] a variety of π units have been reported to be employed to build CMP networks with enhanced π-conjugation in the structure. The resultant CMPs are applied in π-conjugation-favored applications, such as photocatalysis,[68–70] light emittance,[71–73] chemical sensing,[78–81] and energy storage.[82–87] As for the accessible synthesis of monomers, the method of constructing CMPs using the Suzuki–Miyaura cross-coupling reaction has to be stated because of its commercial availability for monomers and wide functional group compatibility, which facilitates the development of the family of functional CMPs. The Suzuki–Miyaura cross-coupling reaction was first reported in 1979 as an outstanding method to link aryl groups;[88,89] and the introduction of the Suzuki–Miyaura cross-coupling reaction to the construction of CMP network accelerates the discovery of diverse advanced applications of CMPs with various choices of functionalized building units.

To obtain the specific functionalities in CMP networks, the appropriate methods for inducing functional groups to the skeleton of CMPs are significant. The most commonly used methods are *de novo* synthesis for building monomers and post-synthetic modifications for the resultant backbone, which are also widely utilized in the functionalization of other porous materials, such as MOFs[90,91] and COFs.[92,93] Both methods exhibit effective functionalization of CMPs but employ different strategies to attach functional groups or active sites to networks of CMP. *De novo* synthesis is a bottom-up strategy that ensures the highest degree of grafting in resultant CMPs according to the design principles for the target applications, whereas, post-synthetic modifications tailor a CMP network that was already been synthesized. Post-synthetic modification is a hugely popular method to functionalize CMPs, as it provides a versatile tool to create a variation of the pristine CMPs with identical spatial structures. This modification is also referred to as post-synthetic functionalization, although allows for diverse functionalities of CMPs, it might bring the unexpected structural collapse of CMPs. Thus, deliberate consideration for the functionalization of CMPs through post-synthetic modification would be especially important while tailoring CMP networks without a decrease in structural stability. This method is usually employed when the target CMPs cannot be synthesized *via* the construction of functional monomers, which are difficult to obtain through traditional synthesis routes. In summary, both *de novo* synthesis and post-synthetic modification of CMPs offer decorating techniques for the tailoring of a CMP network with tailored and anticipated properties, which give these porous organic polymers more advanced applications.

2.2 Synthetic methods

2.2.1 *De novo* synthesis. Due to the great diversity of organic synthesis, tremendous potential designs of functionalized monomers provide researchers a huge reserve of building blocks to choose from for the construction of CMP materials. With these monomers of interest in hand, CMPs can be synthesized with different shapes of the pore space and various functionalization of the pore environment according to the requirement of researchers. Utilizing *de novo* synthesis for functionalizing CMPs, a variety of target networks with distinctive active sites have been developed and employed in a range of research fields with challenges.

2.2.1.1 De novo synthesis of π units. De novo synthesis is ideal as it ensures the highest degree of grafting, in regard to this, it is promising in having each monomer unit containing a functional group, at least. The first CMPs were synthesized by Sonogashira–Hagihara cross-couplings, and aryl halides were coupled by alkyne struts, forming rigid porous structures with alkyne knots existing in networks.[40] On this foundation, a range of monomers containing aryl halides with the specific functional group have been designed and applied to construct CMPs, which exhibit enhanced performance in practical applications, such as photocatalysis. To access the goal for improving the performance of photocatalysis in CMPs, Vilela *et al.* in 2013 reported a series of benzothiadiazole-based CMPs, which were synthesized through a palladium-catalyzed Sonogashira–Hagihara cross-coupling (Fig. 2).[94] The synthesized CMPs dispersed in DMF were tested to obtain the UV/Vis spectra in comparison to the benzothiadiazole monomer afterward, representing a large bathochromic shift of around 90 nm in this conjugated network. These results indicate the π-conjugated system of the monomer might be enlarged *via* the poly-coupling reaction. These bifunctional CMPs with an enhanced π-conjugated effect were employed to evaluate their photocatalytic activities, exhibiting obviously improved performance along with the increase of surface areas of these CMPs, although they were constructed by the same block units. The difference in the photocatalytic performance of these CMPs reveals that the increased contact area between catalysts and reactants is another significant factor for improving photocatalytic efficiency besides the enhanced π-conjugation of CMP materials. Soon after, Cooper *et al.* reported the synthesis of two dye-based CMPs with prominent photoredox catalysis, which were
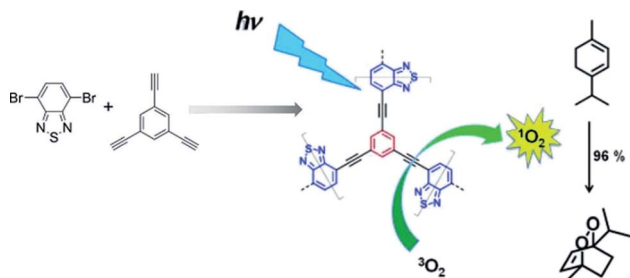
prepared using Rose Bengal dye with 1,4-diethynylbenzene and 1,3,5-triethynylbenzene, respectively as blocking units.[95] The resultant two CMPs, RB-CMP1 and RB-CMP2, both exhibited high conversions and recyclability in aza-Henry reactions as photoredox catalysts. Similarly, Han *et al.* built upon this, demonstrating EY-POPs, which were constructed by the embedding of Eosin Y dye in CMPs *via* a bottom-up strategy.[96] Two EY-POPs were obtained, and 1,3,5-triethynylbenzene and tetra(4-ethynylphenyl)methane were, respectively, used to support Eosin Y dye in the yield π-conjugated networks. These photoactive CMPs reveal high activity and ready recyclability in the aza-Henry reaction. To sum up, this strategy of improving the synergistic effect of active sites and inherent porosities in CMPs has proved to be effective, and is also employed widely in designing other functional porous materials, such as MOFs[97] and COFs.[98,99]

2.2.1.2 De novo metalation of monomers. The Suzuki–Miyaura cross-coupling reaction was utilized in the construction of CMPs subsequently, which advanced the development of functional CMPs because of its commercial availability of monomers and wide functional group compatibility. This reaction, however, has an inevitable shortcoming; it is oxygen-sensitive, which may result in the production of unexpected by-products and decomposition of Pd(0) catalyst. Therefore, the reaction system should be thoroughly degassed while synthesizing such CMPs.[100] Jiang *et al.* demonstrated a light-harvesting conjugated microporous polymer named PP-CMP with 3D polyphenylene scaffolds, which were synthesized by a Suzuki polycondensation reaction in 2010.[101] The success of constructing PP-CMP through the Suzuki cross-coupling reaction led to the diversity of π units and the rapid discovery of such type of CMPs. Bhattacharya *et al.* reported a conjugated donor–acceptor-based bicontinuous microporous networks named Co-MPPy-1, functionalized with a porphyrin unit coordinating with Co(II) ions.[102] Co-MPPy-1 was obtained by the condensation of 1,3,6,8-tetrakis(4,4,5,5-tetramethyl-1,3,2-dioxaborolan-2-yl) pyrene (TBP) and 5,10,15,20-(tetra-4-bromophenyl)porphyrin cobalt(II) (Por-Br) complex through a Pd-mediated Suzuki C–C cross-coupling reaction with a BET surface area of 501 m^2 g^{-1}
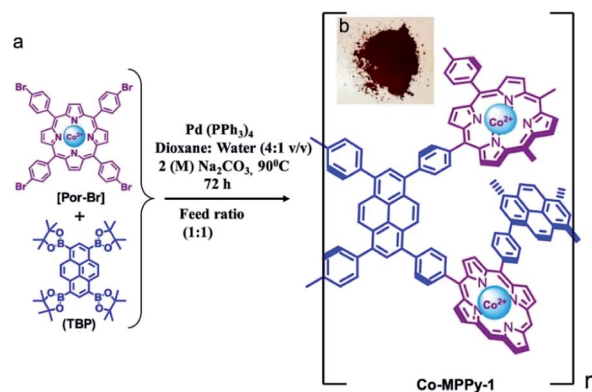

Fig. 2 Synthesis of benzothiadiazole functionalized CMPs. Reproduced with permission.[94] Copyright 2013, John Wiley and Sons.

Fig. 3 Synthesis of metalloporphyrin and pyrene-based CMP, Co-MPPY-1. Adapted with permission.[102] Copyright 2019, American Chemical Society.

(Fig. 3), exhibiting excellent electrochemical activity towards oxygen evolution reaction (OER). The electrochemical oxygen evolution for Co-MPPy-1 and MPPY-1, which were treated in the acid solution to remove all metal sites (Co) from CMP networks were evaluated; Co-MPPy-1 represented superior electrochemical activity compared with MPPY-1. Remote electronic communication between the cobalt(II) porphyrin (donor) to pyrene (acceptor), combining with the efficient charge transport in the Co-MPPy-1 network results in enhanced performance of its catalytic activity. Subsequently, Lan *et al.* nicely demonstrated covalent organic framework nanosheets in highly active electrocatalytic carbon dioxide reduction.[103] They employed the same strategy to enhance the electrocatalytic performances of the catalyst in the CO_2 reduction reaction (CO_2RR). Co-TTCOF, condensed by metalized 5,10,15,20-tetrakis(4-aminophenyl) porphinato (M-TAPP, M = Co here) and 2,3,6,7-tetra(4-formylphenyl)-tetrathiafulvalene (4-formyl-TTF) *via* a Schiff-base reaction, was designed to take advantage of the synergistic combination of metalloporphyrin and TTF. This synergistic effect herein plays a vital role in gathering electron-donating, electron migration, and electrocatalytic active components in the electrocatalytic CO_2RR. With the high porosity, Co-TTCOF also offers a large electrochemical active surface to transport CO_2. Therefore, the appropriate combination of electron donor monomers with electron acceptors might be able to construct intermolecular charge-transfer pathways in the target materials effectively, which could improve the electron transfer efficiency largely, and thereby enhancing the electrocatalytic activity.

The Salen unit with its unique coordination geometry is notable for coordinating a wide variety of metals, which makes it one of the most remarkable ligands in coordination chemistry and catalysis chemistry. Deng *et al.* illustrated the construction of Salen-based CMP materials which could be functionalized by metals of Co and Al, representing high CO_2 uptake ability and effective conversion of CO_2 to propylene carbonate (Fig. 4).[104] To obtain Co-CMP, the dibromo-functionalized precursor monomers (Salen-Co) was first synthesized through a complexation reaction of cobalt acetate $(Co(OAc)_2)$ and (*R*,*R*)-*N*′*N*′-bis(5-bromo-3-*tert*-butyl-salicylidene)-1,2-cyclohexanediaminate (Salen), and then treated with 1,3,5-triethynylbenzene to conjugate monomers *via* the palladium-catalyzed Sonogashira–Hagihara cross-coupling. While, Al-CMP was prepared by the post-modification of Salen-based CMP with $Al(OEt)_3$, and the resonances of the carbonyl functional groups (–C=O) in Al-CMP was similar to that in Co-CMP. The resultant CMP, Co-CMP, has a high BET surface area of 965 m^2 g^{-1} with a good CO_2 uptake of up to 79.3 mg g^{-1}. What is even more interesting is that the Co-CMP displays excellent catalytic activities at atmospheric pressure and room temperature in the fixation of CO_2 to the useful industrial raw material, propylene carbonate, with tetrabutylammonium bromide (TBAB) as a co-catalyst. The example reveals that the bifunctional CMPs, Co-CMP, and Al-CMP, synthesized with the combination of the advantages of high CO_2 uptake and plenty of active catalytic sites, have great potential for practical implementation of CO_2 transformation, and broadening the avenue for designing effective catalysts with
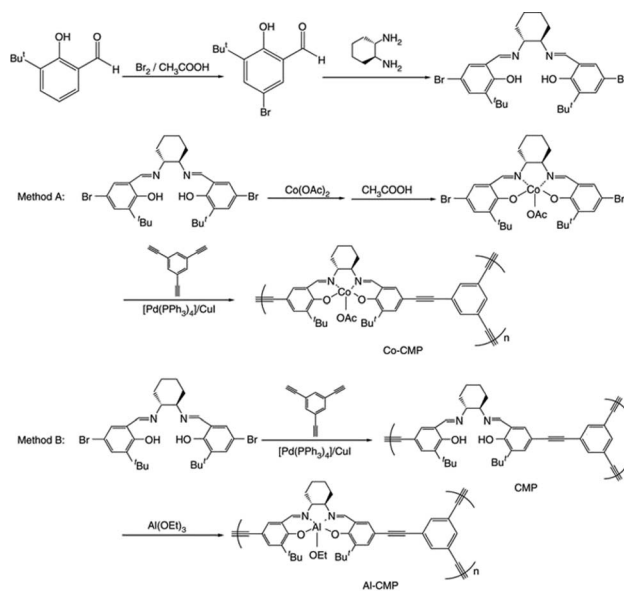

Fig. 4 Synthesis and metalation of Salen-based CMPs, Co-CMP, and Al-CMP. Adapted with permission.[104] Copyright 2013, Nature Publishing Group.

bifunctional active sites, as well. Accordingly, Wang *et al.* reported the first example of a Salen-based COF material. This Salen-COF was obtained from the Schiff-base reaction between 1,3,5-tris[(5-*tert*-butyl-3-formyl-4-hydroxyphenyl)ethynyl] benzene and 1,2-ethylenediamine, which constructed and functionalized the Salen moieties in COF in a single step.[105] Benefiting from a unique coordination geometry of Salen units, a family of metallo-Salen-based COFs can be readily prepared *via* post-synthetic metalation by using different metal ions. The Salen unit as one of the most important ligands in coordination chemistry inevitably not only plays a role in the development of functional porous materials but also pushes forward the applications of such materials due to their structural uniqueness.

2.2.1.3 De novo synthesis of conjugated nodes. Recently, a range of CMPs named as aza-CMPs are produced by the phenazine ring fusion, Jiang *et al.* first described the preparation and energy storage behavior of these CMPs. The aza-fused CMPs were prepared by the fusion of 1,2,4,5-benzenetetramine with triquinoyl hydrate in the presence of $AlCl_3$ at a high temperature in the evacuated ampule and forming 3D ladder CMP networks.[106] This synthesis requires a high reaction temperature, as high as 300–500 °C, which is uneconomical and environmentally unfriendly. To address this problem, Mateo-Alonso's group developed a mild solvothermal method to obtain aza-CMPs by refluxing monomers in the mixture with a rational ratio of the solvent and acetic acid.[107] The aza-CMPs developed by Jiang's group were evaluated for supercapacitive energy storage, which combined the merits of a fused skeleton, dense aza units and well-defined micropores networks, and thus facilitating their electrostatic charge-separation layer formation (Fig. 5). This synergistic effect contained in aza-CMPs reaches the achievement of large capacitance, high energy and power
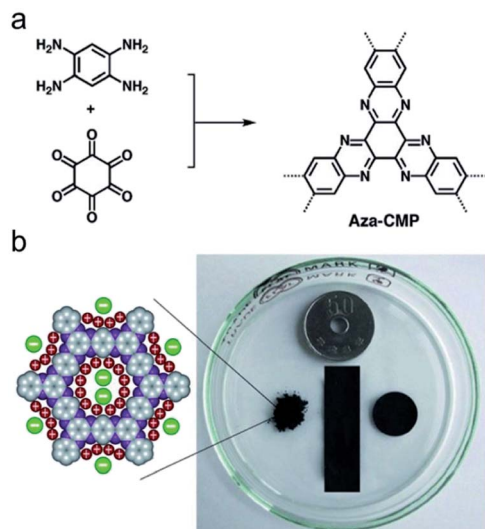
Fig. 5 (a) Synthesis of phenazine–fused aza–CMP and (b) schematic of enhanced electrolyte ions accumulation on the pore walls. Reproduced with permission.[107] Copyright 2013, John Wiley and Sons.

Fig. 6 Synthesis of metal–CMP *via* post–synthetic metalation. Adapted with permission.[114] Copyright 2010, John Wiley and Sons.

densities, and enabling repetitive energy storage and power supply with an excellent life cycle in CMP materials.

2.2.2 Post-synthetic modification. In comparison with *de novo* synthesis, post-synthetic modification (PSM) involves the chemical modification of a CMP network after it has been synthesized, while *de novo* synthesis ensures the highest degree of grafting in the molecule level due to the bottom-up strategy of constructing CMPs. However, with the ease of functionalization of benzene rings that is part of most of the polymers, we can still achieve a very high degree of grafting through post-synthetic modification of CMPs. In 1990, Hoskins and Robson originally proposed the concept of PSM,[108] which was introduced to functionalize MOFs by Wang and Cohen until 2007.[91] Subsequently, this strategy has been widely applied to functionalize all porous materials, including CMPs,[109] POPs,[110] and COFs,[111] due to its convenience. PSM has proven to be a general, practical approach for the functionalization of porous materials after years of practical employment.

2.2.2.1 Post-synthetic metalation. The incorporation of active metal sites into the CMP network can greatly introduce useful chemical functionalities into the pores of CMPs. Some pioneer works have been reported to obtain metal–organic conjugated microporous polymers *via* the support of metalloporphyrin cores in CMP networks, which significantly expand applications of CMPs with the effective combination of chemical and physical properties in the single porous material.[112] Cooper *et al.* described two versatile strategies for constructing metal–organic CMPs (MO-CMPs) without porphyrin-driving monomers (Fig. 6).[113] Compared with the popular MOFs, the metal or metal cluster serves as the linking node to combine inorganic and organic portions in order to establish the open metal–organic framework. The metal sites in the resultant MO-CMPs are no longer needed to connect multiple organic monomers. Rather they are attached to the surface of the CMP skeleton, therefore, allowing the introduction of active metal sites and
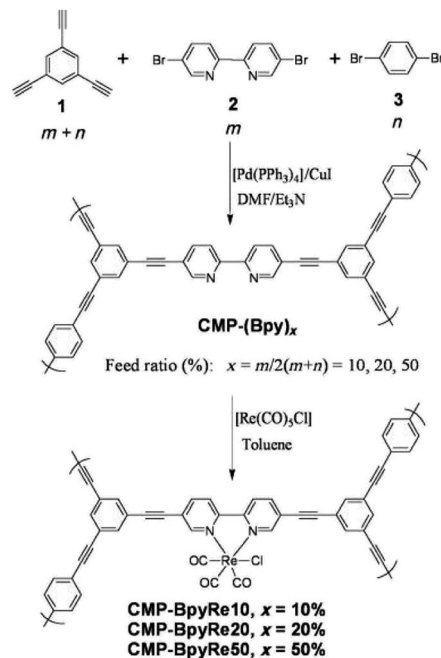
a variety of functionalities without breaking the skeleton. Furthermore, the modification of metal sites after the CMP network being synthesized ensures the maintenance of the extended π-conjugation in CMPs. The CMP-(Bpy)$_x$ was prepared by Sonogashira–Hagihara cross-coupling of 1,3,5-triethynylbenzene with 5,5-dibromo-2,2′-bipyridine and 1,4-dibromobenzene with varying proportions of bipyridines and aromatic groups to manipulate the content of active metal sites in the CMP network. The obtained CMP-(Bpy)$_x$ was treated in the [Re(CO)$_5$Cl] toluene solution to incorporate Re metal sites, and the success of binding Re to the networks was verified by FT-IR spectra compared to the bare CMP-(Bpy)$_x$. Given this, Canivet and co-workers described a family of bipyridine-based CMPs with different loading of Ni metal sites, which were explored for their potential in the catalytic performance of benzothiophene C–H arylation; and the results indicate that these Ni-doped CMPs with abundant active sites possess high catalytic activities and wide scope of applicable substrates.[114] It is obvious that with the aid of post-synthetic modification, we can tune the metal loading in the CMP network precisely and control its chemically active functionalities in accordance with requirements without the damage of the extended π-conjugation in the structure, thereby the high porosity of CMPs is retained, which promises the effective molecule transportation in CMPs after the functionalization.

2.2.2.2 Covalent post-synthetic modification. Apart from the loading of various metal sites in the CMP network to construct bifunctional CMP materials, covalent post-synthetic modification of CMPs is another significant method to alter their chemical and physical properties from pristine CMPs. Over the past few years, comprehensive research on the post-synthetic modification of porous materials has been carried out using

the so-called "click" chemistry, such as azide–alkyne Huisgen cycloaddition[115,116] and thiol–yne click chemistry have been widely used to attach functional groups to the surface of the pores in porous organic materials.[117] Weber *et al.* employed CMP-1 as the template to react with varying amounts of thio-ethanol (C_2SH) or 6-mercaptohexanol (C_6SH) to obtain the resultant CMPs with aliphatic alcohols attached.[118] The radical thiol–yne chemistry of CMPs based on the "click" chemistry of the thiol group and ethynylene units of CMPs would affect the morphology of networks and change the optical properties with different degrees of thiol grafting. While exploring the potential applications of such modified CMPs, Chen *et al.* reported a range of CMPs that the pristine CMP network was treated using various thiol-containing groups.[119] They first synthesized the CMP network, BTT, with the condensation of 4,7-dibromo-benzo[*c*][1,2,5]thiadiazole and 1,3,5-triethynylbenzene *via* a Sonogashira–Hagihara cross-coupling polycondensation, which reacted with the cysteamine in the presence of AIBN in anhydrous DMF at 90 °C for 24 h afterward (Fig. 7). The yielded CMP BTT-SC2NH2 was evaluated on light-driven hydrogen evolution, showing 27.2 times higher performance than that of BBT. In order to verify the accessibility of amino-functionalized CMPs *via* thiol–yne reaction, two more CMPs with enhanced π-conjugation were obtained and treated with cysteamine under the same conditions afterward, named as PB-SC2NH2 and TB-SC2NH2, which were synthesized by 1,4-diethynylbenzene with 1,3,6,8-tetrabromopyrene and 1,1,2,2-tetrakis(4-bromophenyl)ethene, respectively. Both as-prepared CMPs-SC2NH2 showed superior photocatalytic H_2 evolution activity in contrast to the pristine CMPs. Additionally, the hydrogen evolution rate (HER) and apparent quantum yield (AQY) at 420 nm of BTT-SC2NH2 are increased up to 27.2 times and 47.1 times, respectively, compared to BTT without attaching the cysteamine. From this fact, it indicates that the incorporation of amino groups in CMP networks not only increases the hydro-philic surface areas of CMPs-SC2NH2 but also amplifies pho-togenerated charge separation and lengthens electron lifetime, which results in the improvement of the efficiency for subse-quent proton reduction.

Being similar to the thiol–yne click reaction, the amine groups in CMP can be modified to transfer amines into amides by anhydrides with the maintenance of the microporosity, attaching different alkyl chains in the channel surface of CMPs resulting in unique functionalities at the pore surface. Cooper *et al.* demonstrated the synthesis of an amine-functionalized
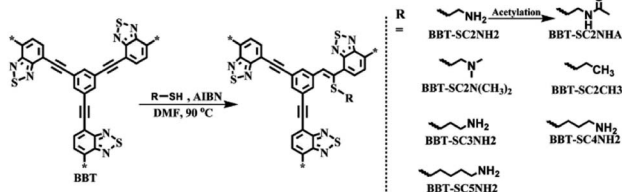

Fig. 8 Synthesis of CMP-1-NH₂ and its post-synthetic modification using anhydrides. Adapted with permission.[120] Copyright 2014, Elsevier Inc.

CMP (CMP-1-NH₂) and its potential to convert to amide-functionalized CMP networks (CMP-1-AMD) *via* the reaction with a series of anhydrides (Fig. 8).[120] CMP-1-AMD was synthe-sized by treating CMP-1-NH₂ directly in the various neat anhy-drides with stirring for 24 h under 30 °C, offering brown powders after washing with $CHCl_3$. With the post-synthetic amidation of CMPs, pore size and pore surface area of CMPs can be controlled by the length and shape of attached alkyl chains, but also the pore environment can be engineered *via* the introduction of a wide range of functionalities. The loading of the chirality to porous materials is a challenging task due to the difficulty in designing chiral monomers, CMP-1-AMD network can serve as a platform to obtain chiral CMPs through the reaction of CMP-1-NH₂ and anhydride with chirality. In brief, the incorporation of pore size and pore surface engineering in CMPs pave the avenue for the next-generation bifunctional CMPs.

The study of CMPs for the adsorption of gases started at an early stage. The well-defined establishment of the structure for CMPs and nicely selected building composition in CMPs offer the opportunity to improve their adsorption capacity and selectivity of a specific gas. In order to enhance the CO_2 sorp-tion, Xu *et al.* introduced metalloporphyrin-based CMPs with the increased electronegativity *via* post-synthetic fluoride func-tionalization.[121] CMP was initially obtained by supporting the core of zinc-porphyrin building block with the mixture of 4,4'-biphenyldiboronic acid and (2,5-bis(azidomethyl)-1,4-phenylene)diboronic acid *via* the Suzuki-coupling reaction. The resultant CMPs then were reacted with 1-ethynyl-2,3,4,5,6-pentafluorobenzene to obtain the fluoride functionalized CMPs through a one-step alkyne–azide coupling reaction using CuI as the catalyst. By controlling the content of azide-containing monomers in CMPs, various target fluoride func-tionalized networks were synthesized and used to evaluate the CO_2 adsorption capacity. It is interesting that the increment of fluoride content in skeletons can significantly increase the CO_2 binding ability and thus improving the CO_2 adsorption capacity. Yet the increased functional groups would lower the porosity of networks significantly and impede further contact with CO_2, and then reduce the CO_2 uptake. Therefore, the collaboration of high surface area and enhanced electronega-tivity of the surface is a promising strategy to discover effective CO_2 adsorbents, providing inspiration for the construction of porous organic materials in the field of gas adsorption.

2.2.2.3 Post-synthetic conversion. Being limited by the complicated synthesis of functional groups in monomers, this

Fig. 7 Synthesis of functionalized BBT *via* thiol–yne click reaction and its possible structures. Adapted with permission.[119] Copyright 2019, Royal Society of Chemistry.
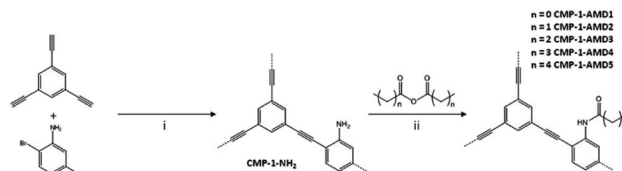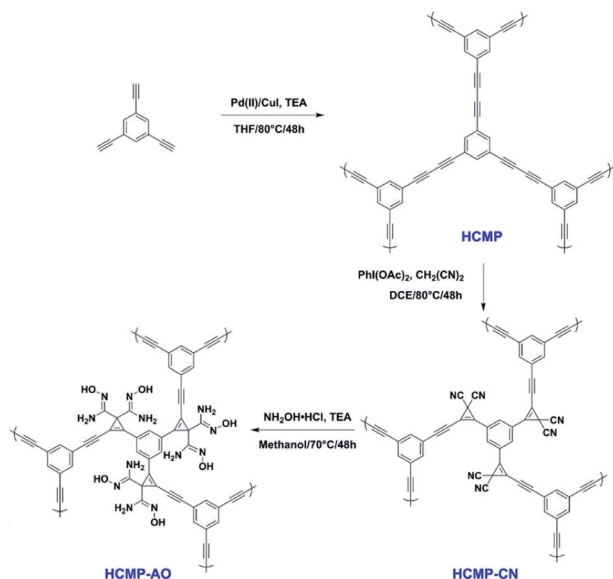
Fig. 9 Synthesis of HCMP-1 functionalized with bis–amidoxime groups. Adapted with permission.[122] Copyright 2020, American Chemical Society.

type of post-synthetic conversion of functionality is extraordinarily helpful for tailoring the pore environment in CMPs for specific applications. In the report published in 2020, we nicely demonstrated a bifunctional CMP adsorbent for the efficient capture of uranium *via* the post-synthetic conversion of functionality.[122] The original CMP was designed by the condensation of a single monomer, 1,3,5-triethynylbenzene, which was then treated with malononitrile to obtain the bis –CN group functionalized CMP networks, HCMP-CN. To improve the uranium binding energy and uptake ability, the –CN group was converted to the amidoxime group, which has a high affinity to uranyl ions (Fig. 9). The evaluation of the adsorption of uranium was investigated in aqueous solutions with the resultant HCMP-AO and showing a much higher adsorption capacity in contrast to that of the original HCMP and HCMP-CN. It indicates that the bis-amidoxime ligands in CMPs contribute to the unique coordination fashion to uranyl ions, suggesting that the synergistic coordination of binding sites can enhance the affinity of chelating groups to the specific ions *via* the improvement of coordinative binding interactions. The strategy we reported would be a promising method to design adsorbents with outstanding capture ability for diverse ionic contaminants, not merely in the adsorption of uranium.

3. Applications of bifunctional CMPs

3.1 Gas storage and separation

Given the unique structure and high porosity, CMPs were initially evaluated for gas storage and separation. CMPs, which are constituted of lightweight elements show great potential for sound gas adsorption capacity and selectivity due to their low density. By means of rational design of building units and synthetic control over structures, the target CMPs can gain improved gravimetric storage capacity. Hydrogen storage has generated great interest in the past few decades due to its potential use as clean energy, and CMPs have been investigated for this objective in their early stage. Cooper *et al.* demonstrated the first application study for CMPs in the field of H_2 storage.[40] It was found that the network with microporosity had an H_2 adsorption capacity of up to 0.99 wt% under the conditions of 77.3 K and 1.13 bar. Another interesting gas storage is the solidification of CH_4 which is an economically attractive fuel, yet the capture and storing of it are full of challenges. HCCP-6 synthesized through the post-synthetic modification from CMP-2 and 1,4-bis(chloromethyl)benzene was evaluated to adsorb CH_4, exhibiting a high CH_4 uptake with a value of 491 mg g^{-1} at 298 K and 80 bars after the molecular expansion of original CMP-2 networks.[123]

Besides the storage of fuel gases, the capture of CO_2, which is the main component of greenhouse gases is also widely studied, and a variety of strategies for enhancing CO_2 uptake of CMPs have been utilized. CMP1, which tuned the pore environment with amine functionalities was employed to explore its potential in CO_2 sorption capacities, representing a modest CO_2 uptake of 1.18 mmol g^{-1} at 298 K and 1 bar.[124] Later, Han *et al.* reported a microporous perfluorinated CTF with the BET surface area of 1535 m^2 g^{-1} revealing a high CO_2 uptake of 3.41 mmol g^{-1} at 298 K and 1 bar,[125] which benefited from the combination of high surface area and electronegative pore environment of this so-called FCTF-1-600 (Fig. 10).

3.2 Heterogeneous catalysis

The open network of CMPs allows easy access of molecules to transport inner channels of pores, which can be used to increase the enrichment of reactants surrounding catalytic sites, thus improving the catalytic efficiency. Jiang *et al.* reported the first iron-based porphyrin CMP network named Fe-CMP with a high BET surface area of 1270 m^2 g^{-1} and plenty of catalytic metalloporphyrin sites, which was synthesized by the polycondensation of iron(III) tetrakis(4'-bromophenyl) porphyrin and 1,4-phenyldiboronic acid *via* a Suzuki–Miyaura cross-coupling reaction.[112] FeP-CMP showed highly active oxidation capability for sulfide groups with chemoselectivity, and the conversion was as high as 99% with a large turnover number (TON = 97 320) (Fig. 11). The bifunctional CMP network, FeP-CMP, bearing a high density of catalytic sites in
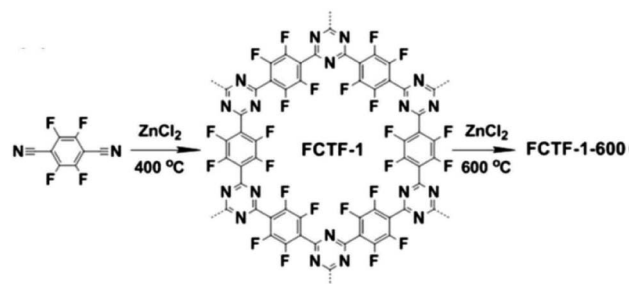

Fig. 10 Synthesis of FCTF with high electronegativity. Adapted with permission.[125] Copyright 2013, Royal Society of Chemistry.
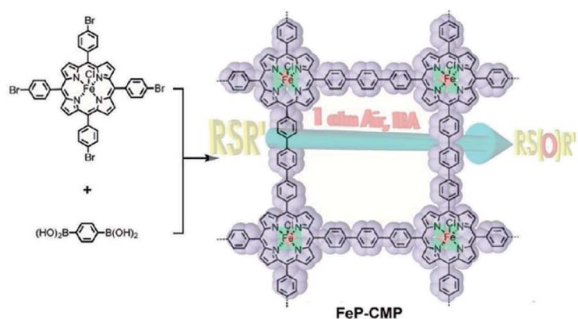
Fig. 11 Synthesis of the nano-heterogeneous catalyst with metalloporphyrin built-in skeleton (FeP-CMP). Reproduced with permission.[112] Copyright 2010, American Chemical Society.

the skeleton and convenient transportation of reactants with high porosity, accelerates the efficiency of catalysis greatly. Therefore, this strategy of constructing an efficient catalysis system provides a blueprint for the further design of a catalyst beginning from the molecular level.

In addition to the introduction of metal catalytic sites in CMPs to build up a catalyst system, the organic functional group can also serve as the active sites to address the challenging catalytic tasks. Wang et al. demonstrated a bifunctional acidic solid catalyst, PPhen-SO$_3$H, which was obtained through the attachment of –SO$_3$H groups to the polyphenylene (PPhen) framework via a post-synthetic modification.[126] PPhen-SO$_3$H featuring high porosity and unique structure ensures the high accessibility of reactants to the active sites, representing enhanced activity in the hydration of alkynes with the combination of the solvation environments in the structure.

3.3 Photocatalysis

Inspired by the extended π-conjugated networks of CMPs, it is believed that CMPs can be employed for photocatalysis after nice tuning of their building units or structures. Vilela et al. reported the synthesis for CMPs with the tailoring of specific electronic properties in the network, which were then evaluated for the activation of singlet oxygen with the conversion of the substrate up to 90%.[94] Shortly after their publication, this CMP was medicated by 3-mercaptopropionic acid through thiol–yne click reaction to convert it from hydrophobicity to hydrophilicity.[127] This modification allows the so-called WCMP to possess higher aqueous compatibility, which promises higher conversion of the substrate in the presence of water, in contrast to the original CMPs.

CMPs bearing the feasibility of wide and tunable band gap would be potential candidates for the photocatalytic generation of H$_2$ from water, and many studies have focused on CMPs in this application.[128–132] Cooper et al. described a library of pyrene-based CMPs with tunable optical gap via the rational copolymerization of benzene- and pyrene-based monomers, which exhibited great potential advantages for water splitting to generate H$_2$.[133] Recently, Jiang and coworkers reported a series of D–π–A CMPs and evaluated their photocatalytic activities for hydrogen evolution from water.[134] The so-called PyBS polymers

were obtained by the condensation of 1,4-benzenediboronic acid bis(pinacol)ester (DBABz) as the π-bridge and varying ratio of 1,3,6,8-tetrabromopyrene (TBrPy) (electron donor) and 3,7-dibromodibenzothiophene-S,S-dioxide (DBrBTDO) (electron acceptor) via a Suzuki–Miyaura cross-coupling reaction. Accordingly, the resultant D–π–A CMPs with different chemical compositions of electron donor and acceptor showed diverse photocatalytic activities for H$_2$ generation. Interestingly, the hydrogen evolution rate (HER) for D–π–A CMPs keeps increasing at first along with the increase of the content of electron acceptor but starts decreasing when the molar percentage of electron acceptor in the generated CMP skeleton is over 75%, demonstrating the significance of the rational assembly of electron acceptor and donor in CMP networks to obtain the optimized photocatalytic activity for hydrogen evolution. The resulting PyBS-3 (donor/acceptor: 25/75) combined broad light adsorption region with high hydrophilicity revealed the highest HER among a total 4 PyBSs, and an HER of 1.05 mmol h^{-1} was observed by 10 mg PyBS-3 under UV/Vis light irradiation with Pt as the co-catalyst and ascorbic acid as the sacrificial hole-scavenger.

Besides photocatalytic water splitting to generate H$_2$, CO$_2$ capture and its photoreduction to useful industrial raw materials is another potential application of bifunctional CMPs.[135–137] Liu and co-workers demonstrated the synthesis of several Eosin Y-functionalized CMPs and their photocatalytic activities in CO$_2$ photoreduction.[138] PEosinY-1 prepared by the Eosin Y and 1,4-diethynylbenzene in the presence of tetrakis(triphenylphosphine)palladium and cuprous iodide had a BET surface area of 445 m^2 g^{-1} with the best performance for the CO$_2$ photoreduction under visible-light irradiation, affording 92% selective reduction for CO combining with a production rate up to 33 μmol g^{-1} h^{-1}.

Except for the introduction of units with specific electronic properties to the network backbone, the position of these substitutions is also crucial in the design of an effective CMP-based photocatalyst. A family of CMPs with the same photocatalytic sites was introduced by Zhang et al., which were constructed by altering the functionality positions on the core phenyl unit (Fig. 12).[139] With the strategy of fine-tuning substitution, the resulting valence and conduction levels of CMP networks can be configured optimally according to the requirement for the specific reductive and oxidative potentials needed in the catalytic system, without the molecular change of the electron donor and acceptor moieties in CMP networks. The designed photocatalyst with substitution on the 1,3,5-positions of the phenyl core exhibited exceptional better photocatalytic activity in the oxidative coupling of benzylamines.

3.4 Light emittance

The restriction for the rotation of phenyl rings in the CMP network avoids fluorescent quenching, which is very common in the π-conjugated linear polymers. Thus, CMPs can be prepared as luminescent materials with rigid and interlocked building blocks. Cooper et al. first reported that the bandgap of CMPs could be tuned by controlling the molecular structure of

Fig. 12 (a) Geometry design principle of valence and conduction band position modification. (b) Synthesis of CMPs with the substitution position modification. Reproduced with permission.[139] Copyright 2015, John Wiley and Sons.

building units.[140] Jiang *et al.* later demonstrated a strategy to construct highly luminescent CMPs through the rational architecture of conjugated building blocks.[141] TPE-CMPs were synthesized using tetrakis(4-bromophenyl)ethene (TBTPE) as a single component *via* the Yamamoto coupling reaction under different reaction times from 2 to 72 h (Fig. 13). The BET surface areas for TPE-CMPs increase along with the increment of the coupling time, meaning that the TPE-CMPs network can grow larger after a longer reaction time and produce higher surface areas without the change of pore size distribution. In comparison with the TBTPE monomer, all TPE-CMP networks showed an absorption band with red-shift, suggesting the π-conjugation extension in the interlocked skeletons with the restricted rotation of phenyl units. Furthermore, TPE-CMPs kept strong luminescence in a wide range of common solvents, showing high applicability. The strategy of confining π-conjugated units in the backbone of CMPs not only promotes the π-electronic conjugation but also facilitates exciton migration in CMPs, which indeed extends the development of luminescent materials with bifunctionalities.

3.5 Environmental remediation

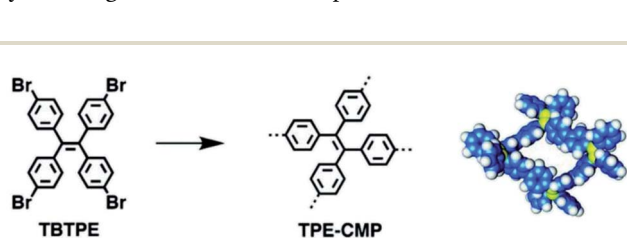The remediation for unclear wastes is a great challenge nowadays. A large number of solid-phase adsorbents have been

applied in this field to eliminate unclear contaminations, including metal–organic frameworks,[142] porous organic polymers,[143,144] and covalent organic frameworks.[145] To enhance the uptake ability, the rational construction of CMPs at the molecular units and pore structure is necessary. Our group reported a bifunctional CMP network owning highly efficient uranium capture *via* the deliberate introduction of synergistic coordination sites to the skeleton.[122] The affinity of chelating groups to uranyl is improved greatly with the increasing coordinative binding interactions after bis-amidoxime functionalized groups have been attached to the backbone of CMPs. Additionally, to amplify coordinative binding interactions, we also designed a CMP network with amidoxime and amine groups (CMP-*m*AO-*o*NH$_2$),[146] which exhibited increased uranium adsorption capacity to 174 mg g^{-1} in contrast to that of amidoxime functionalized CMP network (CMP-*m*AO) without amine groups (105 mg g^{-1}). From these results, it proves that the synergistic coordination to uranyl with the assistance of electron-donating amino functionalities located on the *ortho*-position to the amidoxime groups can greatly improve the performance of amidoxime-based adsorbents for uranium uptake.

The long-lived radioactive iodine (^{129}I or ^{131}I) is a persistent problem, which can be generated from the fume emission of nuclear power plants with grave public health consequences. Thus, the development of adsorbents with fast and efficient capture of iodine and ready recycling ability is urgent. Faul *et al.* introduced a family of hexaphenylbenzene-based CMPs with the construction of a hexakis(4-bromophenyl)benzene (HBB) core and various aryl diamine linkers (HCMPs).[147] These CMPs with moderate surface areas and uniform pore shapes ensure the accessibility of iodine molecules (Fig. 14). HCMP-3 was synthesized with HBB and *o*-tolidine under an N$_2$ atmosphere, exhibiting the highest iodine capture of up to 316 wt% (3.16 g g^{-1}) among these HCMPs, which benefited from the combination of its microporosity with abundant amine functionality in the pore surface providing enough π-electrons. Thus, this synergistic effect endows HCMP-3 with well-defined host–guest interactions, improving the iodine capture with control.

3.6 Chemical sensing

Jiang *et al.* synthesized a highly luminescent CMP with the polycondensation of 3,8,13-tribromo-5,10,15-triethyltriindole (TCB) monomer that could be used to detect arene vapors (Fig. 15).[148] TCB-CMP possessing a large pore surface area

Fig. 13 Synthesis of TPE–CMP with a closed tetragonal skeleton. Reproduced with permission.[141] Copyright 2011, American Chemical Society.
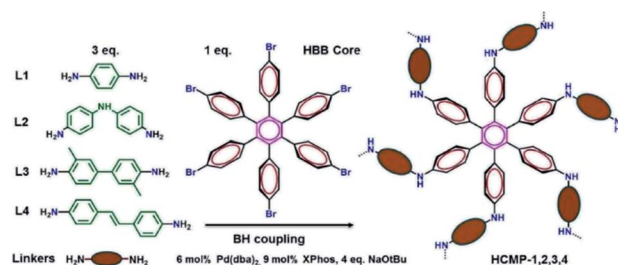

Fig. 14 Synthesis of hexaphenylbenzene-based CMPs. Adapted with permission.[147] Copyright 2016, American Chemical Society.

Fig. 15 Synthesis of carbazole-based CMP (TCB-CMP) and schematic of its sensing mechanism. Reproduced with permission.[148] Copyright 2012, American Chemical Society.

contacting with arenes and photoluminescence properties originating from its π-conjugated skeleton exhibited fast response times and high sensitivity to arenes. Interestingly, TCB-CMP represents superior fluorescence enhancement when contacting electron-rich arene vapors, while drastic fluorescence quenching happens when detecting electron-deficient arene vapors.

Dichtel *et al.* reported a CMP that had fluorescence quenching ability when exposed to 2,4,6-trinitrotoluene (TNT) vapor.[149] The resultant CCP-3 containing 4-dialkoxybenzene substitution was prepared in DMF *via* a Sonogashira–Hagihara cross-coupling reaction and activated by freeze-drying, which had the highest electronic complementarity to TNT vapors with plenty of π-electron-rich units containing in the skeleton. The success of the combination of high porosity and electron-rich system in CCP-3 suggests that CMP possesses promising applications in detecting low-volatility explosives, such as TNT, with the elaborative design of CMP architecture.

3.7 Energy storage

CMPs featuring extended π-conjugated skeletons with permanent micropores are a collection of high-profile porous organic electrode materials in the field of energy storage. A supercapacitor is a type of high-capacity capacitor with a considerably higher capacitance value, storing more than 10 times the charge compared to common capacitors. They are widely used in the area, which requires a rapid response for charge/discharge cycles with long-term persistence. In this regard, the high surface areas of CMPs combined with dense active sites allow the fast transportation of charge from the electrolyte to be stored on the edge of the electronic surface, which makes CMPs a candidate for next-generation supercapacitors. Furthermore, the ready synthesis of building blocks and easy modification of skeleton ensure high tunability of the chemical and physical properties of CMPs, leading to the sophisticated introduction of redox-active sites to the network with interesting and advantageous properties. In addition, the design principle of batteries is similar to that of supercapacitors. The low conductivity of CMPs, however, is of great challenge which limits their real-life implementation in the field of energy storage, and many efforts have been put forward to address this issue in the past few years.

The first report of aza-fused CMPs for supercapacitive energy storage was described by Jiang group.[106] They designed a type of CMPs with N-rich property which was linked together by the phenazine ring fusion under high temperature. Interestingly, the resultant CMP networks are conductive, and the microporosity of CMP results in more surface for electric double-layer capacitance (EDLC) by increasing electrolyte diffusion. Moreover, the aza units in the skeleton enhance the dipolar interactions with the cations of electrolytes, thereby improving proton accumulation on the electronic surface. With the synergistic effect of porosity and the introduction of redox-active sites, the aza-fused CMPs demonstrate distinctive performance for supercapacitive energy storage. The highest capacitance tested under galvanostatic charge–discharge cycling experiments of 0.1 A g^{-1} was reported as 946 F g^{-1} for the aza-CMP, which was synthesized at 450 °C with the BET surface area of 1086 m^2 g^{-1}. Cooper *et al.* recently demonstrated a 2D porous carbon material containing sp^2-hybridized carbons, which were synthesized by the condensation of a single monomer, 3-(dibromomethylene)penta-1,4-diyne, using a Sonogashira–Hagihara cross-coupling reaction, while they were supposed to obtain graphyne-type material initially.[150] The yield 2D-PCM with the unique π-conjugation and hierarchical pore structure was evaluated as an electrode in supercapacitors, showing outstanding electrochemical performance with a capacitance of 378 F g^{-1} at a current density of 0.1 A g^{-1} from galvanostatic charge–discharge cycling experiments.

The first example of a CMP as a cathode in a coin cell was introduced by Jiang and co-workers.[151] A N-rich CMP network, by condensing 1,4-diethynylbenzene and 2,3,8,9,14,15-hexaiododiquinoxalino[2,3-*a*:2′,3′-*c*]phenazine (HIQP), was newly synthesized to qualify the prerequisite as a cathode in Li-ion battery, that is, combining plenty of redox-active sites in the skeleton to store energy with high surface area to maximize charge transportation aiding in easy accessibility to lithium ions. The exploration for the obtained HATN-CM in the application of rechargeable lithium batteries was carried out as a cathode in a coin cell at a current density of 100 mA g^{-1}. HATN-CM exhibited an initial capacity of 147 mA h g^{-1} from the discharge curve when the working potential of HATN-CMP changed from the range 1.5 to 4.0 V *versus* Li/Li$^+$, achieving 71% capability of the theoretical capacity, which was higher than that of monomeric HATN equipped as a cathode (56%). The results obtained from the charge–discharge tests reveal that the CMP skeleton with high porosity enhances the accessibility of redox-active sites for dipolar interactions with the cations, thus improving the performance of energy storage.

Wang *et al.* demonstrated the first example of crystalline CTF used in Li–S batteries.[152] They prepared the material by the condensation of 1,4-dicyanobenzene in the presence of molten ZnCl$_2$ at 400 °C, then loading sulfur into the backbone of CTF-1 through a conventional melting-diffusion method to form the composite material with 34% sulfur loaded according to the weight (Fig. 16a). The performance of galvanostatic measurements for CTF-1/S@155 °C was tested at a current rate of 0.1C, revealing a high discharge capacity of 1197 mA h g^{-1} at the 2nd cycle with relatively good recyclability. The capacity was
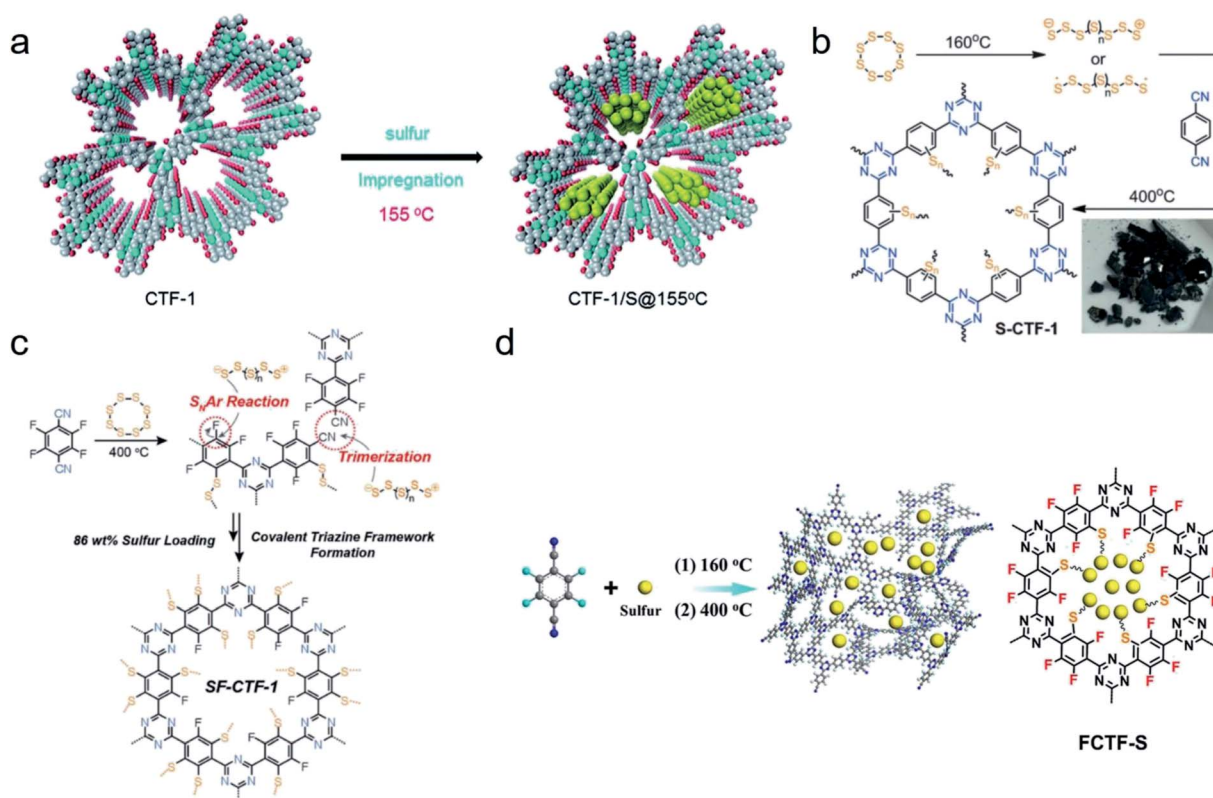
Fig. 16 (a) Synthesis of sulfur-containing CTF-1 by impregnation of molten sulfur. Reproduced with permission.[152] Copyright 2014, Royal Society of Chemistry. (b) Synthesis of S–CTF-1 from elemental sulfur *in situ* and (c) synthesis of SF–CTF-1 involving elemental sulfur-mediated nitrile trimerization along with the simultaneous covalent attachment of elemental sulfur *via* S_NAr chemistry. Reproduced with permission.[153,154] Copyright 2016 and 2017, John Wiley and Sons. (d) Synthesis of the FCTF–S composite by one-step sulfur-assisted cyclotrimerization of aromatic nitriles. Reproduced with permission.[155] Copyright 2017, American Chemical Society.

decreased to 762 mA h g^{-1} after 50 cycles test with a lower coulombic efficiency of 97%. The strategy of designing a sulfur cathode by attaching sulfur to the skeleton using CTF as a host evokes further discovery of constructing suitable CTFs, which can serve as a qualified cathode material in Li–S battery. Coskun and coworkers reported a sulfur-mediated CTF-1, which was synthesized by the cyclotrimerization of 1,4-dicyanobenzene in the presence of elemental sulfur at 400 °C *in situ*.[153] Sulfur polymerization/insertion happened simultaneously with the CTF framework formation, resulting in a uniform distribution of sulfur with a high loading of 62 wt% (Fig. 16b). The original capacity of S–CTF-1 was determined from the potential range 1.7 to 2.7 V *versus* Li/Li$^+$ at 0.05C, as high as 670 mA h g^{-1}. The cooperation of the well-confined sulfur species within the pore porosity and extended π-conjugated skeletons ensures excellent charge conductivity. However, the increment of sulfur content in S–CTF-1 is still inhibited by the crosslinking chemistry of sulfur, which is addressed by Coskun[154] and Wang *et al.*[155] independently through the simultaneous construction of fluorinated CTF and sulfur-mediated trimerization of tetrafluorophthalonitrile soon later (Fig. 16c and d). In this formation, the highly electronegative fluorine atoms in skeletons strengthen the anchoring effect for polysulfides, thereby accelerating the polysulfide conversion and increasing the sulfur content.

4. Outlooks and conclusions

CMPs as a member of the family of porous organic polymers bear unique π-conjugated skeletons with permanent micropores, which ensure them to be a type of high-profile porous material, making a difference to many fields of science and technology. In this review, we described a small portion of the progress in the study of rational design and synthesis for bifunctional CMPs with their advanced applications. The demand for the discovery of real-life implementation of CMPs motivates researchers to optimize the design and functionalization with improved accessibility, which profoundly accelerates the flourish of the field of porous organic polymers. Based on the knowledge of constructing functionality in porous material in the past few years, researchers have developed various methods to functionalize CMPs of interest, including *de novo* synthesis of monomers and post-synthetic modification of CMP networks, which expand the CMP family with unique, sophisticated, and well-designed applications.

As a platform for designing bifunctional porous organic polymers, CMPs enable the introduction of synergistic systems in the skeleton *via* convenient methods and scalable synthesis. This strategy has proven as a useful toolbox for tailoring the functionality of CMP networks, especially in fields such as the

enhancement of light-harvesting, introduction of catalytic centers, and development of electronic redox-active sites.

A small fraction of other bifunctional porous organic polymers has also been covered regarding the design and synthesis of synergistic systems in the skeleton, such as COFs. Additionally, the differences between two functionalizing methods, *de novo* synthesis, and post-synthetic modification, have been discussed with the comparison of grafting degree, synthetic complexity, and functional diversity.

Compared with crystalline covalent organic frameworks, CMPs as amorphous porous organic polymers could be synthesized *via* simpler and more diverse methods without the consideration of obtaining crystalline structures. However, the surface area of the amorphous CMP would be lower than its COF equivalent and the property of conjugation would also be affected if amorphous, thus influencing the practical performance of CMPs. It is believed that the low crystalline order of CMPs would limit their applications, especially after the successful introduction of conjugated COFs, which combine the π-conjugation with crystalline structure in the single skeleton. Such conjugated COFs usually have better BET surface areas and length of conjugation, revealing greater potential than their analogous CMPs. Cooper *et al.* reported their research about crystalline and amorphous CMPs with the same chemical composition for comparison.[156] Unsurprisingly, the conjugated COF demonstrated a better photocatalytic HER performance than that of its analogous disordered CMPs. But most of the crystalline COFs are not stable after being treated in a harsh environment; and their performance would decrease along with the loss of crystallinity, while CMPs with rigid structures and disordered networks would have better recyclability and consistency in real-life implementation. To solve this problem, some strategies have been employed recently to increase the stability of COFs and to improve their recyclability in rigorous working conditions.[157–160] So, what is the selling point for CMPs in comparison with COF actually?

Given the discussion of applications of the above-mentioned bifunctional CMPs, a unique selling point would be their extended conjugation in the skeleton and various adaptations for conjugation enhancement. Thus, those applications favouring these properties would take advantage of CMPs and benefit from their unique conjugated structures. Such as photocatalysis, batteries and energy storage. A lot of CMPs have been applied to study photoredox catalysis, including photocatalytic oxygen activation, photocatalytic water splitting, and CO_2 photoreduction. Although the development of CMPs in this area has been proceeding for several years, it is still worth exploring because of the expanded photoredox catalysis, such as complex organic synthesis. Traditionally, most photoredox catalysts would contain transition metals but CMPs offer the opportunity to reduce the use of expensive metals and improve operational reliability and recyclability. Additionally, the band gap of CMPs could be tuned precisely and easily *via* many methods to fit the requirements of specific photoredox catalysis, making CMP more versatile in multiple applications. Another research area worth exploring for CMPs is batteries and energy storage, the bulk conductivity of most of CMPs, however,

limits their capabilities in such areas. Therefore, developing CMPs with better conductivity rather than mixing with other conductive materials in use is still a long way to go. We believe CMPs would play a significant role in those challenging tasks after addressing the problems above.

Conflicts of interest

There are no conflicts to declare.

Acknowledgements

Notes and references

1 R. M. Barrer, *Zeolites*, 1981, **1**, 130–140.
2 R. Fricke, H. Kosslick, G. Lischke and M. Richter, *Chem. Rev.*, 2000, **100**, 2303–2406.
3 Y. Wan and D. Zhao, *Chem. Rev.*, 2007, **107**, 2821–2860.
4 Z. A. Alothman, *Materials*, 2012, **5**, 2874–2902.
5 H. Furukawa, K. E. Cordova, M. O'Keeffe and O. M. Yaghi, *Science*, 2013, **341**, 1230444.
6 H.-C. Zhou and S. Kitagawa, *Chem. Soc. Rev.*, 2014, **43**, 5415–5418.
7 S. Kitagawa, R. Kitaura and S.-i. Noro, *Angew. Chem., Int. Ed.*, 2004, **43**, 2334–2375.
8 W. Lu, Z. Wei, Z.-Y. Gu, T.-F. Liu, J. Park, J. Park, J. Tian, M. Zhang, Q. Zhang, T. Gentle III, M. Bosch and H.-C. Zhou, *Chem. Soc. Rev.*, 2014, **43**, 5561–5593.
9 J. R. Long and O. M. Yaghi, *Chem. Soc. Rev.*, 2009, **38**, 1213–1214.
10 M. O'Keeffe, *Chem. Soc. Rev.*, 2009, **38**, 1215–1217.
11 O. K. Farha and J. T. Hupp, *Acc. Chem. Res.*, 2010, **43**, 1166–1175.
12 O. M. Yaghi, M. O'Keeffe, N. W. Ockwig, H. K. Chae, M. Eddaoudi and J. Kim, *Nature*, 2003, **423**, 705–714.
13 B. Chen, S. Xiang and G. Qian, *Acc. Chem. Res.*, 2010, **43**, 1115–1124.
14 A. P. Côté, A. I. Benin, N. W. Ockwig, M. O'Keeffe, A. J. Matzger and O. M. Yaghi, *Science*, 2005, **310**, 1166.
15 C. S. Diercks and O. M. Yaghi, *Science*, 2017, **355**, eaal1585.
16 X. Feng, X. Ding and D. Jiang, *Chem. Soc. Rev.*, 2012, **41**, 6010–6022.
17 S.-Y. Ding and W. Wang, *Chem. Soc. Rev.*, 2013, **42**, 548–568.
18 N. Huang, P. Wang and D. L. Jiang, *Nat. Rev. Mater.*, 2016, **1**, 16068.
19 P. Kuhn, M. Antonietti and A. Thomas, *Angew. Chem., Int. Ed.*, 2008, **47**, 3450–3453.
20 P. Katekomol, J. Roeser, M. Bojdys, J. Weber and A. Thomas, *Chem. Mater.*, 2013, **25**, 1542–1548.
21 Z. Yang, H. Chen, S. Wang, W. Guo, T. Wang, X. Suo, D. E. Jiang, X. Zhu, I. Popovs and S. Dai, *J. Am. Chem. Soc.*, 2020, **142**, 6856–6860.

22 C. Krishnaraj, H. S. Jena, K. Leus and P. Van Der Voort, *Green Chem.*, 2020, **22**, 1038–1071.

23 M. Liu, L. Guo, S. Jin and B. Tan, *J. Mater. Chem. A*, 2019, **7**, 5153–5172.

24 S. Das, P. Heasman, T. Ben and S. L. Qiu, *Chem. Rev.*, 2017, **117**, 1515–1563.

25 W. Ji, T.-X. Wang, X. Ding, S. Lei and B.-H. Han, *Coord. Chem. Rev.*, 2021, **439**, 213875.

26 P. Kaur, J. Hupp and S. T. Nguyen, *ACS Catal.*, 2011, **1**, 819–835.

27 Y. Zhang and S. N. Riduan, *Chem. Soc. Rev.*, 2012, **41**, 2083–2094.

28 V. A. Davankov and M. P. Tsyurupa, *React. Polym.*, 1990, **13**, 27–42.

29 L. X. Tan and B. Tan, *Chem. Soc. Rev.*, 2017, **46**, 3322–3356.

30 J. Huang and S. R. Turner, *Polym. Rev.*, 2017, **6**, 1–41.

31 N. Fontanals, R. M. Marce, F. Borrull and P. A. G. Cormack, *Polym. Chem.*, 2015, **6**, 7231–7244.

32 T. Ben, H. Ren, S. Ma, D. Cao, J. Lan, X. Jing, W. Wang, J. Xu, F. Deng, J. M. Simmons, S. Qiu and G. Zhu, *Angew. Chem., Int. Ed.*, 2009, **48**, 9457–9460.

33 Y. Tian and G. Zhu, *Chem. Rev.*, 2020, **120**, 8934–8986.

34 Y. Yuan and G. Zhu, *ACS Cent. Sci.*, 2019, **5**, 409–418.

35 T. Ben and S. Qiu, *CrystEngComm*, 2013, **15**, 17–26.

36 A. I. Cooper, *Adv. Mater.*, 2009, **21**, 1291–1295.

37 Y. Xu, S. Jin, H. Xu, A. Nagai and D. Jiang, *Chem. Soc. Rev.*, 2013, **42**, 8012–8031.

38 J.-S. M. Lee and A. I. Cooper, *Chem. Rev.*, 2020, **120**, 2171–2214.

39 N. Chaoui, M. Trunk, R. Dawson, J. Schmidt and A. Thomas, *Chem. Soc. Rev.*, 2017, **46**, 3302–3321.

40 J. X. Jiang, F. B. Su, A. Trewin, C. D. Wood, N. L. Campbell, H. J. Niu, C. Dickinson, A. Y. Ganin, M. J. Rosseinsky, Y. Z. Khimyak and A. I. Cooper, *Angew. Chem., Int. Ed.*, 2007, **46**, 8574–8578.

41 G. Cheng, T. Hasell, A. Trewin, D. J. Adams and A. I. Cooper, *Angew. Chem., Int. Ed.*, 2012, **51**, 12727–12731.

42 P. Pallavi, S. Bandyopadhyay, J. Louis, A. Deshmukh and A. Patra, *Chem. Commun.*, 2017, **53**, 1257–1260.

43 B. Huang, P. Zhao, Y. Dai, S. Deng and A. Hu, *J. Polym. Sci., Part A: Polym. Chem.*, 2016, **54**, 2285–2290.

44 R. Chinchilla and C. Nájera, *Chem. Soc. Rev.*, 2011, **40**, 5084–5121.

45 A. Suzuki, *Angew. Chem., Int. Ed.*, 2011, **50**, 6723–6737.

46 A. Suzuki, *Chem. Commun.*, 2005, 4759–4763.

47 T. Yamamoto, A. Morita, Y. Miyazaki, T. Maruyama, H. Wakayama, Z.-h. Zhou, Y. Nakamura and T. Kanbara, *Macromolecules*, 1992, **25**, 1214–1223.

48 I. P. Beletskaya and A. V. Cheprakov, *Chem. Rev.*, 2000, **100**, 3009–3066.

49 S.-L. You, Q. Cai and M. Zhang, *Chem. Soc. Rev.*, 2009, **38**, 2190–2201.

50 T. B. Poulsen and K. A. Jørgensen, *Chem. Rev.*, 2008, **108**, 2903–2915.

51 J. K. Stille and E. Mainen, *J. Polym. Sci., Part B: Polym. Lett.*, 1966, **4**, 39–41.

52 J. K. Stille and E. L. Mainen, *Macromolecules*, 1968, **1**, 36–42.

53 W. Shi, C. Liu and A. Lei, *Chem. Soc. Rev.*, 2011, **40**, 2761–2776.

54 E. H. Cordes and W. P. Jencks, *J. Am. Chem. Soc.*, 1962, **84**, 832–837.

55 J. L. Segura, M. J. Manchenõa and F. Zamora, *Chem. Soc. Rev.*, 2016, **45**, 5635–5671.

56 V. Gevorgyan and Y. Yamamoto, *J. Organomet. Chem.*, 1999, **576**, 232–247.

57 S. Kotha, E. Brahmachary and K. Lahiri, *Eur. J. Org. Chem.*, 2005, 4741–4767.

58 C. Zhang, X. Yang, Y. Zhao, X. Wang, M. Yu and J.-X. Jiang, *Polymer*, 2015, **61**, 36–41.

59 Q. Shi, H. Sun, R. Yang, Z. Q. Zhu, W. Liang, D. Tan, B. Yang, A. Li and W. Deng, *J. Mater. Sci.*, 2015, **50**, 6388–6394.

60 P. Lindemann, M. Tsotsalas, S. Shishatskiy, V. Abetz, P. Krolla-Sidenstein, C. Azucena, L. Monnereau, A. Beyer, A. Gölzhäuser, V. Mugnaini, H. Gliemann, S. Bräse and C. Wöll, *Chem. Mater.*, 2014, **26**, 7189–7193.

61 D. Z. Tan, W. J. Fan, W. N. Xiong, H. X. Sun, A. Li, W. Q. Deng and C. G. Meng, *Eur. Polym. J.*, 2012, **48**, 705–711.

62 W. Lu, Z. Wei, D. Yuan, J. Tian, S. Fordham and H.-C. Zhou, *Chem. Mater.*, 2014, **26**, 4589–4597.

63 Y. Xie, T. T. Wang, R. X. Yang, N. Y. Huang, K. Zou and W. Q. Deng, *ChemSusChem*, 2014, **7**, 2110–2114.

64 Y.-B. Zhou and Z.-P. Zhan, *Chem.–Asian J.*, 2018, **13**, 9–19.

65 Y. Z. Liao, Z. H. Cheng, W. W. Zuo, A. Thomas and C. F. J. Faul, *ACS Appl. Mater. Interfaces*, 2017, **9**, 38390–38400.

66 S. Tantisriyanurak, H. N. Duguid, L. Peattie and R. Dawson, *ACS Appl. Polym. Mater.*, 2020, **2**, 3908–3915.

67 X. Wang, S.-M. Lu, J. Li, Y. Liu and C. Li, *Catal. Sci. Technol.*, 2015, **5**, 2585–2589.

68 N. Kang, J. H. Park, K. C. Ko, J. Chun, E. Kim, H.-W. Shin, S. M. Lee, H. J. Kim, T. K. Ahn, J. Y. Lee and S. U. Son, *Angew. Chem., Int. Ed.*, 2013, **52**, 6228–6232.

69 Z. J. Wang, S. Ghasimi, K. Landfester and K. A. I. Zhang, *Chem. Commun.*, 2014, **50**, 8177–8180.

70 Z. J. Wang, S. Ghasimi, K. Landfester and K. A. I. Zhang, *Chem. Mater.*, 2015, **27**, 1921–1924.

71 X. Liu, Y. Zhang, H. Li, A. Sigen, H. Xia and Y. Mu, *RSC Adv.*, 2013, **3**, 21267–21270.

72 P. Zhang, K. Wu, J. Guo and C. Wang, *ACS Macro Lett.*, 2014, **3**, 1139–1144.

73 B. Bonillo, R. S. Sprick and A. I. Cooper, *Chem. Mater.*, 2016, **28**, 3469–3480.

74 A. Sigen, Y. Zhang, Z. Li, H. Xia, M. Xue, X. Liu and Y. Mu, *Chem. Commun.*, 2014, **50**, 8495–8498.

75 T. M. Geng, Z. M. Zhu, W. Y. Zhang and Y. Wang, *J. Mater. Chem. A*, 2017, **5**, 7612–7617.

76 Y. Liu, Y. Cui, C. Zhang, J. Du, S. Wang, Y. Bai, Z. Liang and X. Song, *Chem.–Eur. J.*, 2018, **24**, 7480–7488.

77 M. Xu, T. Wang, P. Gao, L. Zhao, L. Zhou and D. Hua, *J. Mater. Chem. A*, 2019, **7**, 11214–11222.

78 L. Sun, Z. Liang, J. Yu and R. Xu, *Polym. Chem.*, 2013, **4**, 1932–1938.

79 L. B. Sun, Y. C. Zou, Z. Q. Liang, J. H. Yu and R. R. Xu, *Polym. Chem.*, 2014, **5**, 471–478.

80 T. M. Geng, H. Zhu, W. Song, F. Zhu and Y. Wang, *J. Mater. Sci.*, 2016, **51**, 4104–4114.

81 Z. Li, Y. Zhi, X. Feng, X. Ding, Y. Zou, X. Liu and Y. Mu, *Chem.–Eur. J.*, 2015, **21**, 17355–17362.

82 X. Zhuang, F. Zhang, D. Wu, N. Forler, H. Liang, M. Wagner, D. Gehrig, M. R. Hansen, F. Laquai and X. Feng, *Angew. Chem., Int. Ed.*, 2013, **52**, 9668–9672.

83 H. Zhang, Y. Zhang, C. Gu and Y. Ma, *Adv. Energy Mater.*, 2015, **5**, 1402175.

84 Q. Zhang, S. Ge, X. Wang, H. Sun, Z. Zhu, W. Liang and A. Li, *RSC Adv.*, 2014, **4**, 41649–41653.

85 S. Zhang, W. Huang, P. Hu, C. Huang, C. Shang, C. Zhang, R. Yang and G. Cui, *J. Mater. Chem. A*, 2015, **3**, 1896–1901.

86 C. Zhang, Y. He, P. Mu, X. Wang, Q. He, Y. Chen, J. Zeng, F. Wang, Y. Xu and J. Jiang, *Adv. Funct. Mater.*, 2018, **28**, 1705432.

87 K. Ding, Q. Liu, Y. Bu, K. Meng, W. Wang, D. Yuan and Y. Wang, *J. Alloys Compd.*, 2016, **657**, 626–630.

88 N. Miyaura, K. Yamada and A. Suzuki, *Tetrahedron Lett.*, 1979, **20**, 3437–3440.

89 N. Miyaura and A. Suzuki, *J. Chem. Soc., Chem. Commun.*, 1979, 866–867.

90 A. Kirchon, L. Feng, H. F. Drake, E. A. Joseph and H.-C. Zhou, *Chem. Soc. Rev.*, 2018, **47**, 8611–8638.

91 Z. Wang and S. M. Cohen, *J. Am. Chem. Soc.*, 2007, **129**, 12368–12369.

92 Y. Song, Q. Sun, B. Aguila and S. Ma, *Adv. Sci.*, 2018, **6**, 1801410.

93 Y. Yusran, X. Guan, H. Li, Q. Fang and S. Qiu, *Natl. Sci. Rev.*, 2020, **7**, 170–190.

94 K. Zhang, D. Kopetzki, P. H. Seeberger, M. Antonietti and F. Vilela, *Angew. Chem., Int. Ed.*, 2013, **52**, 1432–1436.

95 J.-X. Jiang, Y. Li, X. Wu, J. Xiao, D. J. Adams and A. I. Cooper, *Macromolecules*, 2013, **46**, 8779–8783.

96 C.-A. Wang, Y.-W. Li, X.-L. Cheng, J.-P. Zhang and Y.-F. Han, *RSC Adv.*, 2017, **7**, 408–414.

97 T. Zhang and W. Lin, *Chem. Soc. Rev.*, 2014, **43**, 5982–5993.

98 M. Bhadra, S. Kandambeth, M. K. Sahoo, M. Addicoat, E. Balaraman and R. Banerjee, *J. Am. Chem. Soc.*, 2019, **141**, 6152–6156.

99 W. Li, X. Huang, T. Zeng, Y. A. Liu, W. Hu, H. Yang, Y. B. Zhang and K. Wen, *Angew. Chem., Int. Ed.*, 2021, **60**, 1869–1874.

100 Q. Liu, Z. Tang, M. Wu and Z. Zhou, *Polym. Int.*, 2014, **63**, 381–392.

101 L. Chen, Y. Honsho, S. Seki and D. Jiang, *J. Am. Chem. Soc.*, 2010, **132**, 6742–6748.

102 S. Bhunia, K. Bhunia, B. C. Patra, S. K. Das, D. Pradhan, A. Bhaumik, A. Pradhan and S. Bhattacharya, *ACS Appl. Mater. Interfaces*, 2019, **11**, 1520–1528.

103 H.-J. Zhu, M. Lu, Y.-R. Wang, S.-J. Yao, M. Zhang, Y.-H. Kan, J. Liu, Y. Chen, S.-L. Li and Y.-Q. Lan, *Nat. Commun.*, 2020, **11**, 497.

104 Y. Xie, T. T. Wang, X. H. Liu, K. Zou and W. Q. Deng, *Nat. Commun.*, 2013, **4**, 1960.

105 L.-H. Li, X.-L. Feng, X.-H. Cui, Y.-X. Ma, S.-Y. Ding and W. Wang, *J. Am. Chem. Soc.*, 2017, **139**, 6042–6045.

106 Y. Kou, Y. Xu, Z. Guo and D. Jiang, *Angew. Chem., Int. Ed.*, 2011, **50**, 8753–8757.

107 A. B. Marco, D. Cortizo-Lacalle, I. Perez-Miqueo, G. Valenti, A. Boni, J. Plas, K. Strutynski, S. De Feyter, F. Paolucci, M. Montes, A. N. Khlobystov, M. Melle-Franco and A. Mateo-Alonso, *Angew. Chem., Int. Ed.*, 2017, **56**, 6946–6951.

108 B. F. Hoskins and R. Robson, *J. Am. Chem. Soc.*, 1990, **112**, 1546–1554.

109 Y. Y. Cui, C. X. Yang and X. P. Yan, *ACS Appl. Mater. Interfaces*, 2020, **12**, 4954–4961.

110 Y. Zhang and S. N. Riduan, *Chem. Soc. Rev.*, 2012, **41**, 2083–2094.

111 J. L. Segura, S. Royuela and M. M. Ramos, *Chem. Soc. Rev.*, 2019, **48**, 3903–3945.

112 L. Cheng, Y. Yang and D. Jiang, *J. Am. Chem. Soc.*, 2010, **132**, 9138–9143.

113 J. X. Jiang, C. Wang, A. Laybourn, T. Hasell, B. Clowes and A. I. Cooper, *Angew. Chem., Int. Ed.*, 2011, **50**, 1072–1075.

114 Y. Mohr, M. Alvas-Favaro, R. Rajapaksha, G. Hisler, A. Ranscht, P. Samanta, C. Lorentz, M. Duguet, C. Mellot-Draznieks, E. A. Quadrelli, F. M. Wisser and J. Canivet, *ACS Catal.*, 2021, **11**, 3507–3515.

115 A. Nagai, Z. Guo, X. Feng, S. Jin, X. Chen, X. Ding and D. Jiang, *Nat. Commun.*, 2011, **2**, 536.

116 H. Xu, J. Gao and D. L. Jiang, *Nat. Chem.*, 2015, **7**, 905–912.

117 Q. Sun, B. Aguila, J. Perman, L. D. Earl, C. W. Abney, Y. Cheng, H. Wei, N. Nguyen, L. Wojtas and S. Ma, *J. Am. Chem. Soc.*, 2017, **139**, 2786–2793.

118 B. Kiskan and J. Weber, *ACS Macro Lett.*, 2012, **1**, 37–40.

119 X. Wang, X. Zhao, W. Dong, X. Zhang, Y. Xiang, Q. Huang and H. Chen, *J. Mater. Chem. A*, 2019, **7**, 16277–16284.

120 T. Ratvijitvech, R. Dawson, A. Laybourn, Y. Z. Khimyak, D. J. Adams and A. I. Cooper, *Polymer*, 2014, **55**, 321–325.

121 D. Cui, C. Yao and Y. Xu, *Chem. Commun.*, 2017, **53**, 11422–11425.

122 L. Zhang, N. Pu, B. Yu, G. Ye, J. Chen, S. Xu and S. Ma, *ACS Appl. Mater. Interfaces*, 2020, **12**, 3688–3696.

123 Y. Liu, S. Wang, X. Meng, Y. Ye, X. Song, Z. Liang and Y. Zhao, *Angew. Chem., Int. Ed.*, 2020, **59**, 19487–19493.

124 R. Dawson, D. J. Adams and A. I. Cooper, *Chem. Sci.*, 2011, **2**, 1173–1177.

125 Y. Zhao, K. X. Yao, B. Teng, T. Zhang and Y. Han, *Energy Environ. Sci.*, 2013, **6**, 3684–3692.

126 Y. Liu, B. Wang, L. Kang, A. Stamatopoulos, H. Gu and F. R. Wang, *Chem. Mater.*, 2020, **32**, 4375–4382.

127 H. Urakami, K. Zhang and F. Vilela, *Chem. Commun.*, 2013, **49**, 2353–2355.

128 R. S. Sprick, B. Bonillo, M. Sachs, R. Clowes, J. R. Durrant, D. J. Adams and A. I. Cooper, *Chem. Commun.*, 2016, **52**, 10008–10011.

129 L. Wang, Y. Wan, Y. Ding, S. Wu, Y. Zhang, X. Zhang, G. Zhang, Y. Xiong, X. Wu, J. Yang and H. Xu, *Adv. Mater.*, 2017, **29**, 1702428.

130 Z. Wang, X. Yang, T. Yang, Y. Zhao, F. Wang, Y. Chen, J. H. Zeng, C. Yan, F. Huang and J.-X. Jiang, *ACS Catal.*, 2018, **8**, 8590–8596.

131 J. Yu, X. Sun, X. Xu, C. Zhang and X. He, *Appl. Catal., B*, 2019, **257**, 117935.

132 C. Yang, B. C. Ma, L. Zhang, S. Lin, S. Ghasimi, K. Landfester, K. A. I. Zhang and X. Wang, *Angew. Chem., Int. Ed.*, 2016, **55**, 9202–9206.

133 R. Sprick, J. Jiang, B. Bonillo, S. Ren, T. Ratvijitvech, P. Guiglion, M. A. Zwijnenburg, D. J. Adams and A. I. Cooper, *J. Am. Chem. Soc.*, 2015, **137**, 3265–3270.

134 C. Shu, C. Han, X. Yang, C. Zhang, Y. Chen, S. Ren, F. Wang, F. Huang and J.-X. Jiang, *Adv. Mater.*, 2021, **33**, 2008498.

135 F. M. Wisser, P. Berruyer, L. Cardenas, Y. Mohr, E. A. Quadrelli, A. Lesage, D. Farrusseng and J. Canivet, *ACS Catal.*, 2018, **8**, 1653–1661.

136 C. Yang, W. Huang, L. C. da Silva, K. A. I. Zhang and X. Wang, *Chem.–Eur. J.*, 2018, **24**, 17454–17458.

137 C. Dai, L. Zhong, X. Gong, L. Zeng, C. Xue, S. Li and B. Liu, *Green Chem.*, 2019, **21**, 6606–6610.

138 X. Yu, Z. Yang, B. Qiu, S. Guo, P. Yang, B. Yu, H. Zhang, Y. Zhao, X. Yang, B. Han and Z. Liu, *Angew. Chem., Int. Ed.*, 2019, **58**, 632–636.

139 Z. J. Wang, S. Ghasimi, K. Landfester and K. A. I. Zhang, *Adv. Mater.*, 2015, **27**, 6265–6270.

140 J. X. Jiang, A. Trewin, D. J. Adams and A. I. Cooper, *Chem. Sci.*, 2011, **2**, 1777–1781.

141 Y. H. Xu, L. Chen, Z. Q. Guo, A. Nagai and D. Jiang, *J. Am. Chem. Soc.*, 2011, **133**, 17622–17625.

142 H. Zhang, W. Liu, A. Li, D. Zhang, X. Li, F. Zhai, L. Chen, L. Chen, Y. Wang and S. Wang, *Angew. Chem., Int. Ed.*, 2019, **58**, 16110–16114.

143 Q. Sun, L. Zhu, B. Aguila, P. K. Thallapally, C. Xu, J. Chen, S. Wang, D. Rogers and S. Ma, *Nat. Commun.*, 2019, **10**, 1646.

144 Q. Sun, B. Aguila, J. Perman, A. S. Ivanov, V. S. Bryantsev, L. D. Earl, C. W. Abney, L. Wojtas and S. Ma, *Nat. Commun.*, 2018, **9**, 1644.

145 Q. Sun, B. Aguila, L. D. Earl, C. W. Abney, L. Wojtas, P. K. Thallapally and S. Ma, *Adv. Mater.*, 2018, **30**, 1705479.

146 B. Yu, L. Zhang, G. Ye, Q. Liu, J. Li, X. Wang, J. Chen, S. Xu and S. Ma, *Nano Res.*, 2021, **3**, 788–796.

147 Y. Liao, J. Weber, B. M. Mills, Z. Ren and C. F. J. Faul, *Macromolecules*, 2016, **49**, 6322–6333.

148 X. Liu, Y. Xu and D. Jiang, *J. Am. Chem. Soc.*, 2012, **134**, 8738–8741.

149 J. L. Novotney and W. R. Dichtel, *ACS Macro Lett.*, 2013, **2**, 423–426.

150 Y. Xu, R. S. Sprick, N. J. Brownbill, F. Blanc, Q. Li, J. W. Ward, S. Ren and A. I. Cooper, *J. Mater. Chem. A*, 2021, **9**, 3303–3308.

151 F. Xu, X. Chen, Z. Tang, D. Wu, R. Fu and D. Jiang, *Chem. Commun.*, 2014, **50**, 4788–4790.

152 H. Liao, H. Ding, B. J. Li, X. Ai and C. Wang, *J. Mater. Chem. A*, 2014, **2**, 8854–8858.

153 S. N. Talapaneni, T. H. Hwang, S. H. Je, O. Buyukcakir, J. W. Choi and A. Coskun, *Angew. Chem., Int. Ed.*, 2016, **55**, 3106–3111.

154 S. H. Je, H. J. Kim, J. Kim, J. W. Choi and A. Coskun, *Adv. Funct. Mater.*, 2017, **27**, 1703947.

155 F. Xu, S. Yang, G. Jiang, Q. Ye, B. Wei and H. Wang, *ACS Appl. Mater. Interfaces*, 2017, **9**, 37731–37738.

156 X. Wang, L. Chen, S. Y. Chong, M. A. Little, Y. Wu, W.-H. Zhu, R. Clowes, Y. Yan, M. A. Zwijnenburg, R. S. Sprick and A. I. Cooper, *Nat. Chem.*, 2018, **10**, 1180–1189.

157 S. Kandambeth, V. Venkatesh, D. B. Shinde, S. Kumari, A. Halder, S. Verma and R. Banerjee, *Nat. Commun.*, 2015, **6**, 6786.

158 P.-F. Wei, M.-Z. Qi, Z.-P. Wang, S.-Y. Ding, W. Yu, Q. Liu, L.-K. Wang, H.-Z. Wang, W.-K. An and W. Wang, *J. Am. Chem. Soc.*, 2018, **140**, 4623–4631.

159 X. Li, C. Zhang, S. Cai, X. Lei, V. Altoe, F. Hong, J. J. Urban, J. Ciston, E. M. Chan and Y. Liu, *Nat. Commun.*, 2018, **9**, 2998.

160 J. Liu, T. Yang, Z.-P. Wang, P.-L. Wang, J. Feng, S.-Y. Ding and W. Wang, *J. Am. Chem. Soc.*, 2020, **142**, 20956–20961.